F.E. Analysis of Montreal Stadium Roof Under Variable Loading Conditions

Massimiliano LAZZARI
PhD - Civil Engineer
University of Padua
Padua, Italy

Massimo MAJOWIECKI
Assoc. Professor
IUAV - Venice
Venice, Italy

Anna SAETTA
Assoc. Professor
IUAV - Venice
Venice, Italy

Renato VITALIANI
Professor
University of Padua
Padua, Italy

Summary

The roof over the Montreal Stadium is composed of a pre-tensioned membrane combined with an eccentric cable-stayed system. Due to the eccentricity of the cable system, the structure is non-symmetric, which leads to a non-uniform structural response under variable static loads.

This paper begins by analyzing the free vibrations and the frequencies of the structure, then goes on to consider the effects of wind and snow on the Montreal Stadium roof using the geometrically non-linear finite element procedure ("Loki") developed according to the total Lagrangian formulation. The loads induced by wind are simulated as deformation-dependent forces, i.e. follower loads.

Such a refined model, in terms of the representation of both the structure and the load conditions, enables the structural mechanisms that caused the failure of the roof membrane on a number of occasions to be described and better understood.

Keywords: Montreal Stadium roof; wind action; cable-suspended structures; geometrical non-linearity; finite elements; dynamic analysis; time-domain approach.

1. Introduction

The drastic reduction in the ratio of permanent weight to variable load makes lightweight structures particularly sensitive to the effects of wind and snow. The dynamic nature of wind action can cause oscillations and deformations of such amplitude that they jeopardize the function of the roof and, in the worst cases, its structural stability. On the other hand, the static effect of snow represents an extremely heavy load for this type of structure, even reaching as high as 70-80% of the total load. Melchers [1] demonstrated that one of the primary causes of collapse (corresponding to approximately 45% of the cases analyzed) lies in an erroneous evaluation of the loading conditions and of the structural response. With improvements in the methods for in-depth analysis in the design of lightweight wide-span roofing, theoretical studies can and must be used in combination with experimental tests performed in wind tunnels and in situ. From the observation of structures that have completely or partially collapsed:

- due to snow, e.g. the Hartford Coliseum (1978), the Pontiac Stadium (1982), the Milan Sports Hall (1985) and the Montreal Olympic Stadium (1992);
- due to wind, e.g. the Montreal Olympic Stadium (1988);
- due to the effects of water, e.g. the Minnesota Metrodome (1983) inflatable roof

information has been collected and design specifications have been obtained for the verification of such structures in ultimate and serviceability limit states. The difficulties involved in assessing and simulating the real load conditions are described in [2] [3],[4].

The structural problems deriving from the static and frequential analysis of the roof over the Olympic Stadium in Montreal, Canada, subjected to loading by snow and wind, emerge particularly clearly. The aim of the present study was to contribute, both in qualitative and in quantitative terms, towards explaining the failure phenomena that have occurred on several occasions in the roof of the Olympic Stadium in Montreal in apparently unexceptional conditions (Fig. 1). This situation led, in 1992, to the creation of an international committee of experts with a view to arriving at a

preliminary diagnosis of the structural inadequacy of the roofing, clarifying the likely causes of the damage that occurred in the fabric of the roofing membrane. The present study, with a view to providing a complete analytical picture of the roof's static response, will describe both some original contribution and the previously formulated findings and considerations (that may be stressed here, though they were not the object of further analysis).

The committee of experts suggested submitting the roofing to analyses in the non-linear field to test their assumptions and clarify certain aspects under debate. The present study, starting from data on the geometry, materials, and design details provided in [5], proposes a static analysis based on a new numerical model of the structure, comparing and discussing the results, and emphasizing the principal characteristics of the structural response.

The quantities used for the comparison are the data collected in the experts' analysis and the reports produced by certain eye witnesses that describe the failure of the structure. In particular, the observers emphasize how the first collapse (the situation studied in this paper) coincided with a wind of low intensity (approximately 19 m/s) coming to bear at an angle corresponding to approximately 60° between the direction of the wind and the main axis of the roof. Moreover, the structure was characterized prior to collapse by an antimetric dynamic movement with respect to its lesser dimension inducing an oscillation with an amplitude of around 5 meters.

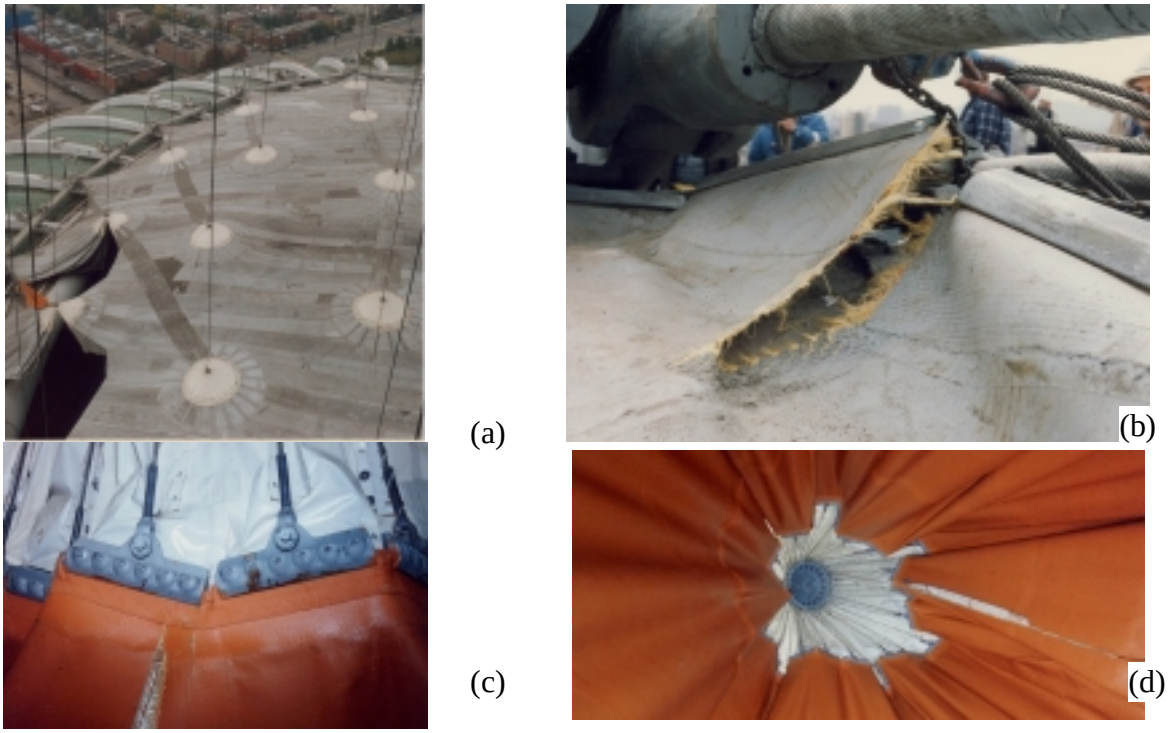

Fig. 1: Membrane failure (a) between the suspension cones, (b) at the edge in the vicinity of the coupling point, and (c) in line with the clamps in the vicinity of the membrane joint.

2. The Structure

The roof over the playing field at the baseball stadium in Montreal is a lightweight structure of the tensegrity system type, with a membrane having a double curvature that covers an ellipse-shaped opening 200 m long and 140 m wide (Fig. 2). The shape of the membrane, which is characterized by a double hyperbolic curvature, was obtained by means of a uniform elliptic pre-stressing, adopting as the geometric boundary conditions an anchorage at 17 points around the perimeter and a suspension from 26 internal points.

The anchorages lie on a steel ring with a hollow rectangular cross-section, whose function is to absorb the circumferential compression that develops as a result of the geometric-stress state of the structure; the ring is fixed to the overhanging edges on the side of the reinforced concrete roof over the stands. A cable along the edge ensures the transfer of the stresses from the membrane to the anchorages.

The 26 internal supporting points are made with a system of suspension cables hanging from the great leaning tower made of steel and concrete that clearly becomes the principal roof-supporting structure, as well as its housing during periods when it is removed. The principal cable and the membrane are connected by interposing 40 slender cables that depart from the main cable along the directrices of a cone, each ending with a clamp that grips the membrane and, through friction, ensures a distributed transfer of the stresses (Fig. 1c).

Horizontal connection cables are then provided between the internal suspension points and between these and the anchorages on the perimeter ring, developing roughly along the horizontal projection of the suspension cables. Their main function is to receive the horizontal component of the resultant of the principal cables, enabling the membrane to take on a suitable shape and adequate prestressing levels.

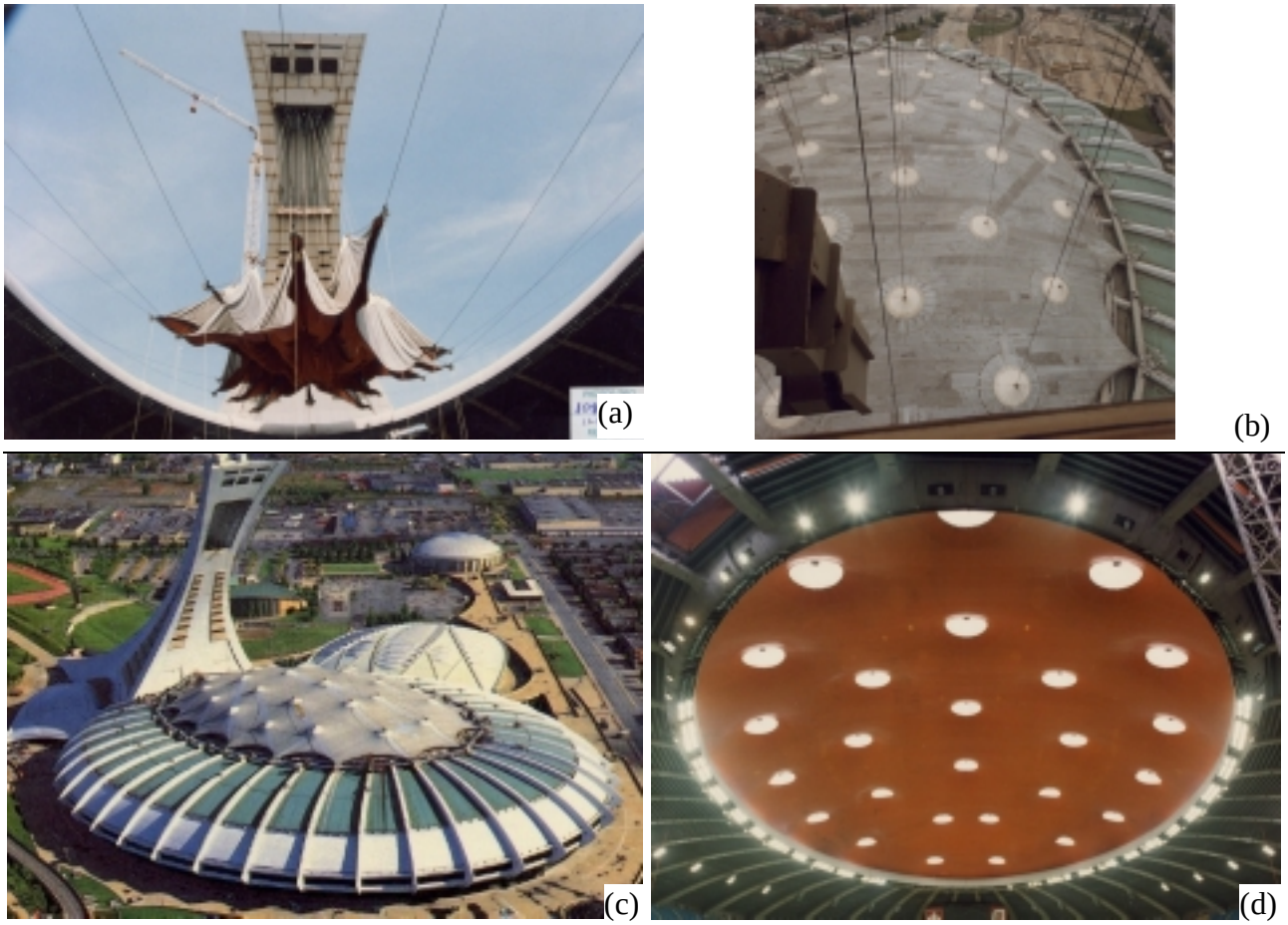

Fig. 2: (a) opening of the membrane, (b) suspension system (suspension cables, connection cables, perimeter cables and membrane), (c) and (d) outside and inside of the roof

2.1 The Materials

Membrane: the membrane is a “Panama” fabric of Kevlar 49 aramidic fibers, 1420 den, coated with PVC type “B 1086” (Verseidag Industrietextilien, Krefeld, Germany), which guarantees a strength of 490 kN/m in the direction of both the warp and the weave.
The actual values measured testify to a much higher strength, around 620-640 kN/m in the direction of the warp and 580 kN/m in the direction of the weave. The modulus of elasticity is E = 16MN/m², in conditions of stress along two axes over an average stress range. To increase the durability of its mechanical characteristics with respect to deterioration due to the environment working conditions, the PVC protective coating was subsequently further coated with a layer of polyurethane that was colored according to the recommendations of the membrane’s manufacturer: the final thickness was 2.5 mm and the self weight 29 N/m². The assembly of the membrane was done using a stitched jointing process with two variants, using 15 and 20 lines of seam, but the stitching was always restricted to not more than two layers of fabric at one time. The edges of the membrane were

finished with a system of aluminum shapes and pairs of steel clamps designed to exert a pinching action on the fabric, thus avoiding the need to resort to punched connections.

Cables: galvanized harmonic steel strands with an open or closed Z-shaped cross-section were used to achieve a system of cables for supporting the structure. The minimum ultimate strength was 1600 N/mm², while the equivalent modulus of elasticity was E = 160000 N/mm². The need to use these cables was dictated by the high loads that would come to bear on the roof, especially the load due to snow.

2.2 The Numerical Model

Numerical model of the structure: the finite element model of the structure (Fig. 3) uses two types of element: four-node membrane elements and two-node cable elements. The characteristics of each of the finite elements implemented in the Loki code are described in [3]. The overall dimensions of the model amounted to 2452 nodal points for 7356 degrees of freedom, on which 868 cable elements and 1937 membrane elements were constructed. The main suspension cables and the connection cables were modeled using 4 cable elements; the cables inserted between the membrane and the suspension and connection cables were described by single cable elements, while the perimeter cables were represented by a number of cables varying between 7 and 9. There were 43 points of restraint amounting to a total restraint of 129 degrees of freedom, while the modeling of the mechanical and material characteristics of the structural components was done using 12 numerical sets for the cables and just one set for the membrane. The material in the numerical simulation was assumed to be elastic linear; non-linear constitutive laws are involved [6].

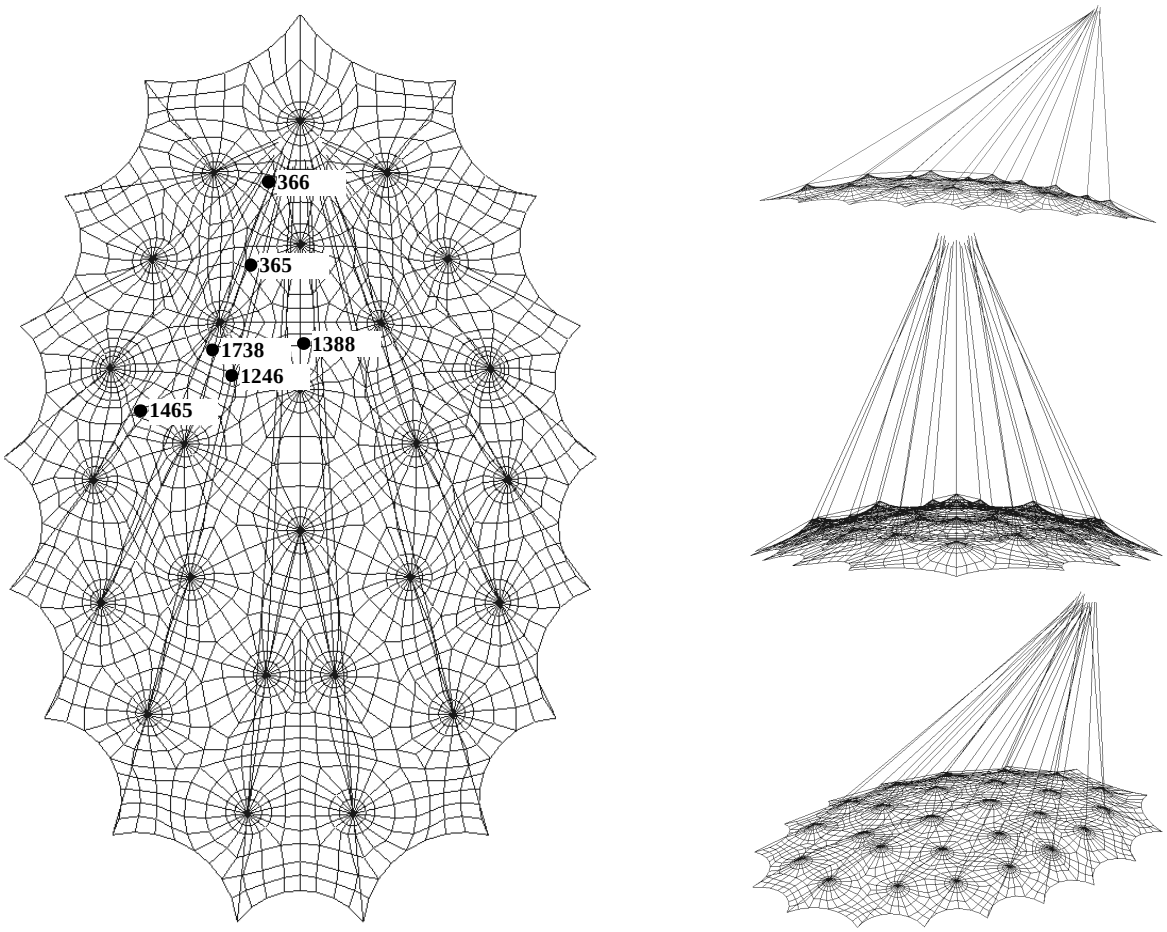

Fig. 3: Finite element model, first roof over the Olympic Stadium in Montreal

Numerical model of the loads: the numerical model of the loads corresponds to conservative surface loads for the simulation of loads due to snow, while the simulation used non-conservative follower loads for a realistic description of wind action [7] [8]. It proves essential to describe the load due to

wind as a follower load because of the considerable displacements that occur in the roofing membrane under varying load conditions, both in the static and in the dynamic field. This description of the load considerably increases the burden of the calculation of the system and makes it necessary to use non-symmetrical solution finders. The self weight of the membrane was 29 N/m², the average prestressing in both directions was 10 kN/m, the average load due to snow 1650 N/m² and the average load due to wind 700 N/m².

3. Static analyses

3.1 '0 state'

The original design idea involved all 26 cables in the operations for lifting and transferring the prestressing forces to the roof. Later on, however, these operations were separated with a view to achieving a greater structural simplicity, so 12 cables were used to transfer the prestressing action and the other 14 served for lifting the membrane. The search for the 0 state was done using the same structural model as the one employed for the analyses under static and dynamic exogenous loads (wind and snow). Given the geometric non-linearity of the problem, the procedure is of the iterative type and the arrangement of the initial configuration is assumed to equate to the final configuration obtained from the previous iteration. This procedure enables the use of the same numerical model to study both the 0 state and the related analyses.

3.1.1 Roofing membrane

The stress level reached by means of the numerical analyses performed with the LOKI indicates a mean final value of 9.9 kN/m. The peak value achieved locally by the prestressing was not considered significant because of a stress concentration at the most critical points due to the discretization of the roofing continuum, which occurs in the portions of membrane in the middle of the cones (Fig. 4).

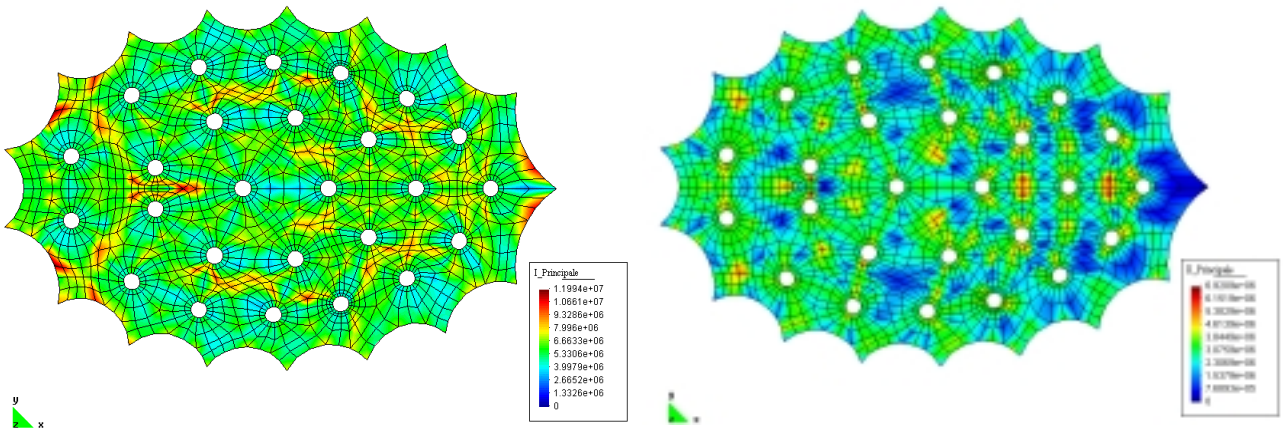

Fig. 4: 1st principal stress and 2nd principal stress

3.1.2 Supporting, Connecting and Perimeter Cables

With reference to the principal supporting cables and to the horizontal connection cables, a comparison is drawn here between the stress levels calculated by prior analyses (performed on a model of the structure with a network of cables [5], and by the numerical model of the present study (developed using the LOKI code). In the same terms, but with regard to the perimeter cables, a comparison is drawn between the stresses calculated in the vicinity of the anchorages on the perimeter ring. The differences are minimal, in relative terms, for the principal cables and the outermost sub-horizontal connection cables (i.e. those connected directly to the anchorages on the perimeter ring), because the design stresses were attributed directly to the numerical model developed for the present study. The stresses on the remainder of the elements derive from the equilibrium established following the solution of the "0 state" and are more sensitive, but in absolute terms these values are far from the allowable limits.

	Cable	Element	Cross section [mm^2]	σ_{LOKI} [N/mm^2]	$\sigma_{REP.}$ [N/mm^2]	Difference %
Suspension cables	1	765 - 766	5219	224.2	226.3	-0.9
	2	773 - 774	5219	67.9	65.8	3.3
	3	781 - 782	5219	140.2	141.7	-1.1
	4	853	4163	50.8	50.6	0.3
	5	789 - 790	4163	56.5	57.1	-1.1
Connection cables	1	653 - 654	5750	269.0	271.3	-0.9%
	2	661 - 662	2875	150.8	146.5	2.9%
	3	669 - 670	731	164.7	147.6	11.5%
	4	760	731	110.9	85.4	29.8%
	5	677 - 678	4188	210.9	211.3	-0.2%
Perimeter cables	1	537 - 538	2875	48.3	62.4	-22.6
	2	521 - 522	2875	89.5	84.5	5.9
	3	589 - 590	2875	71.1	80.2	-11.4
	4	523 - 524	2875	53.9	62.3	-13.5
	5	577 - 578	2875	65.9	57.0	15.6

Table 1 Comparison between the literature [e.g. 5] and the Loki numerical analysis

3.2 Eigenvalue analysis

The eigenvalues were calculated around the situation of equilibrium determined by the prestressing alone and by the gravitational loads. The eigenvectors calculated were arranged in order of increasing frequency; the first 350 were considered, distinguishing them and classifying them in three categories:

- the first category includes the vibration modes that almost exclusively affect the cables;
- the second category comprises the modes in which the vibration of the cables is associated with a relevant vibration of the membrane too;
- the third category includes eigenvectors that mainly affect the membrane, for which the displacement of the cables is virtually negligible.

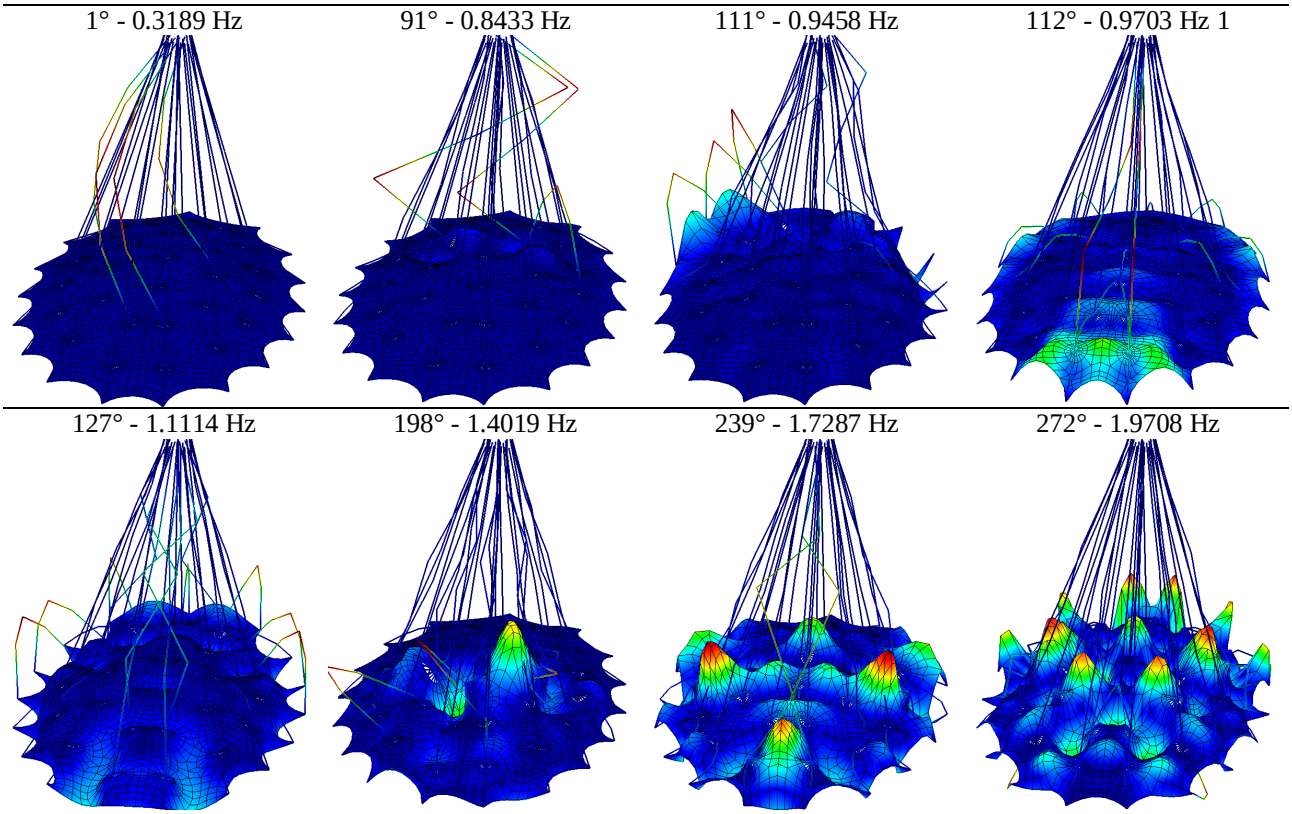

Fig. 5: Eigenvectors and eigenvalues of vibration modes 1 - 272

This distinction is also suggested by the distribution of the eigenvectors of these three categories on the frequency field. Fig. 5 shows the images of a few eigenvectors with their respective eigenvalues to describe the evolution of the vibration modes with increasing frequencies.

The eigenvectors of each category concentrate around certain frequency values, depending on the fundamental harmonic considered.
A first, lower range of frequencies (roughly the first 30) is dominated by vibration modes that fit into the first category; thereafter, vibration modes of the second and subsequently of the third category appear, and their presence becomes progressively stronger. The first consideration stems from the fact that the structure as a whole presents no eigenvectors demonstrating the global involvement typical of the fundamental harmonics. The eigenvectors are frequently expressed at local level, in one or more limited areas separated from other parts of roofing that remain substantially undisturbed. The total involvement of the structure occurs with the higher harmonics.

The exclusive presence of potential vibration modes dominated by the sum of vibrations in limited portions of roofing indicates the scarcely rigid character, or the inadequacy of the pre-stressing of the structure. The analysis of the own modes of vibration under loading conditions (snow and wind) reveals how the global stiffness characteristics change considerably.

3.3 Static Analysis with Snow and Wind

Static analyses were carried out in "*quasi-static*" conditions, dividing the total load into 100 fractions and applying them cumulatively at intervals with a step $\Delta t = 1$ s.
This method was chosen because, in the static analysis, the solution finder was unable to proceed beyond half of the final loading level due to the onset of local buckling effects that prevented its convergence. Generally speaking, the structure demonstrates a marked difference in behavior between the front (the southern side) and the back (northern side), especially as concerns the displacements. In this simulation the effect of earthquake loads has not been considered, since in lightweight structures it is negligible if compared with snow and wind load.

3.3.1 Snow: membrane

The displacements calculated on the membrane were due to its own deformability and partly also to the displacement of the lower ends of the suspension cables. The maximum deflection reaches 4 m at the front, whereas it does not exceed 2.5 m at the back Fig. 6. The discriminant for reaching said values lies in the displacement of the lower ends of the suspension cables. In fact, the membrane - in terms of displacement and stresses - always responds in the same way all over the roof and any variability is due to differences in the span between the various suspension cones.

Such variations tend rather to lead to the formation, in some areas, of "pocket deformations" that favor a local build-up of snow far greater than elsewhere on the roof. The formation of such pockets and the related risk of structural collapse are described in [5] and emphasized as a negative feature of the structural design. The 1st principal stress (Fig. 6d) exceeds 280 kN/m in the areas where the cables of the cones grip the membrane, while it is no more than 200 kN/m in the other areas. Towards the cones there is therefore a concentration of the stresses, also intuitively predicted *a priori*. The 2nd principal stress diminishes over almost all of the membrane as the load increases, to such a degree that already at 8% of the final load we can see ample areas that are no longer stressed, i.e. areas that have lost all their initial pre-stressing. The mapping of the 2nd principal stress is consequently of little significance and emphasizes the scarce structural stiffness of the roofing in relation to the loads due to snow predicted during the design phase. This low structural stiffness derives from the limited contra-curvature with respect to the principal dimensions of the membrane panels coming within the suspension cones. In addition, the membrane suffers excessively from the slanting angle and length of the suspension cables, showing signs of a different behavior at the front by comparison with the back.

3.3.2 Wind: membrane

Unlike the loads due to snow, the effect of wind action causes a part of the roof (to the north) to reveal a pneumatic type of behavior, i.e. the principal cables are unable to work under negative pressure beyond a certain value and the structural displacement takes on the nature of a global ballooning effect (Fig. 7).

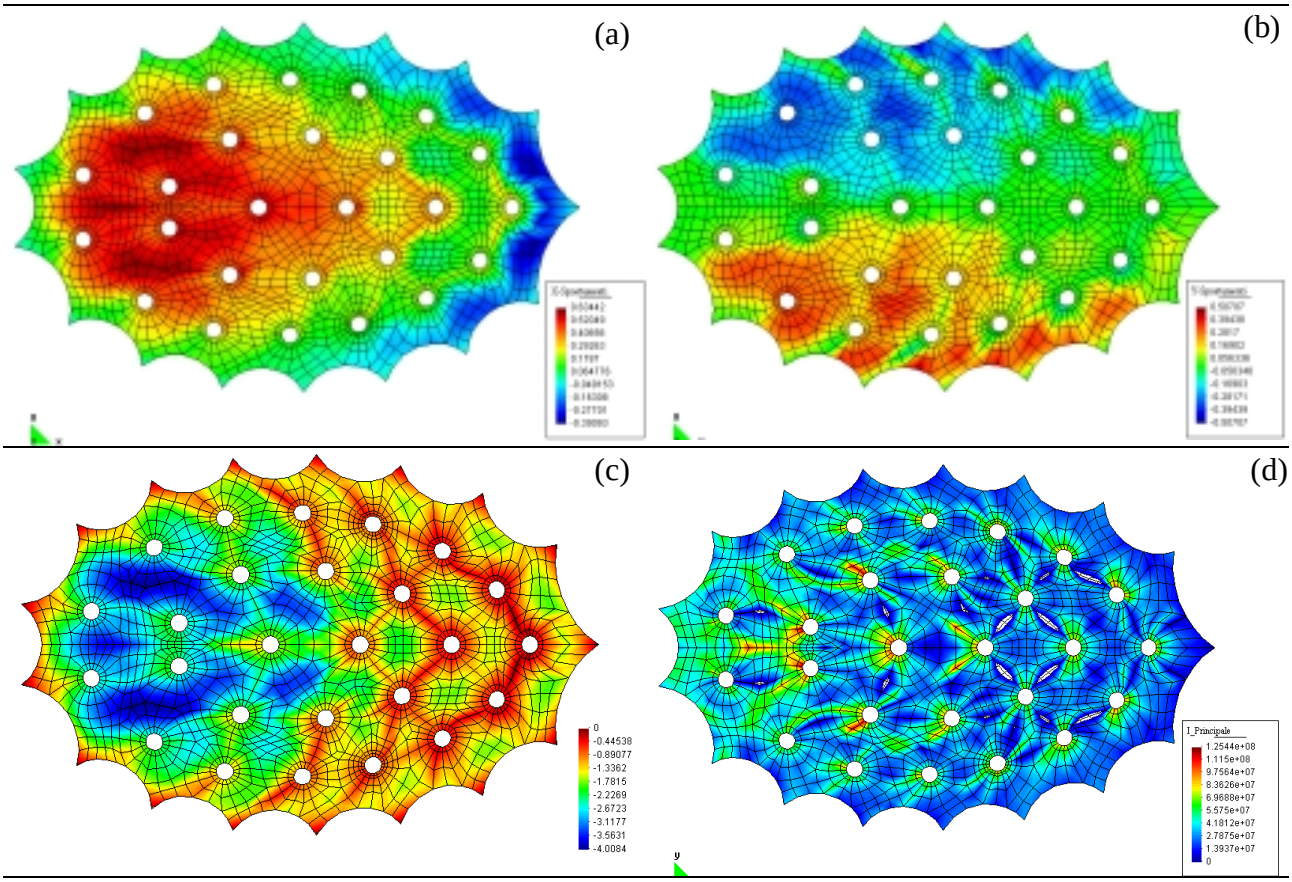

Fig. 6: snow – displacements [m] X, Y and Z [m] and 1st principal stresses [N/mm²]

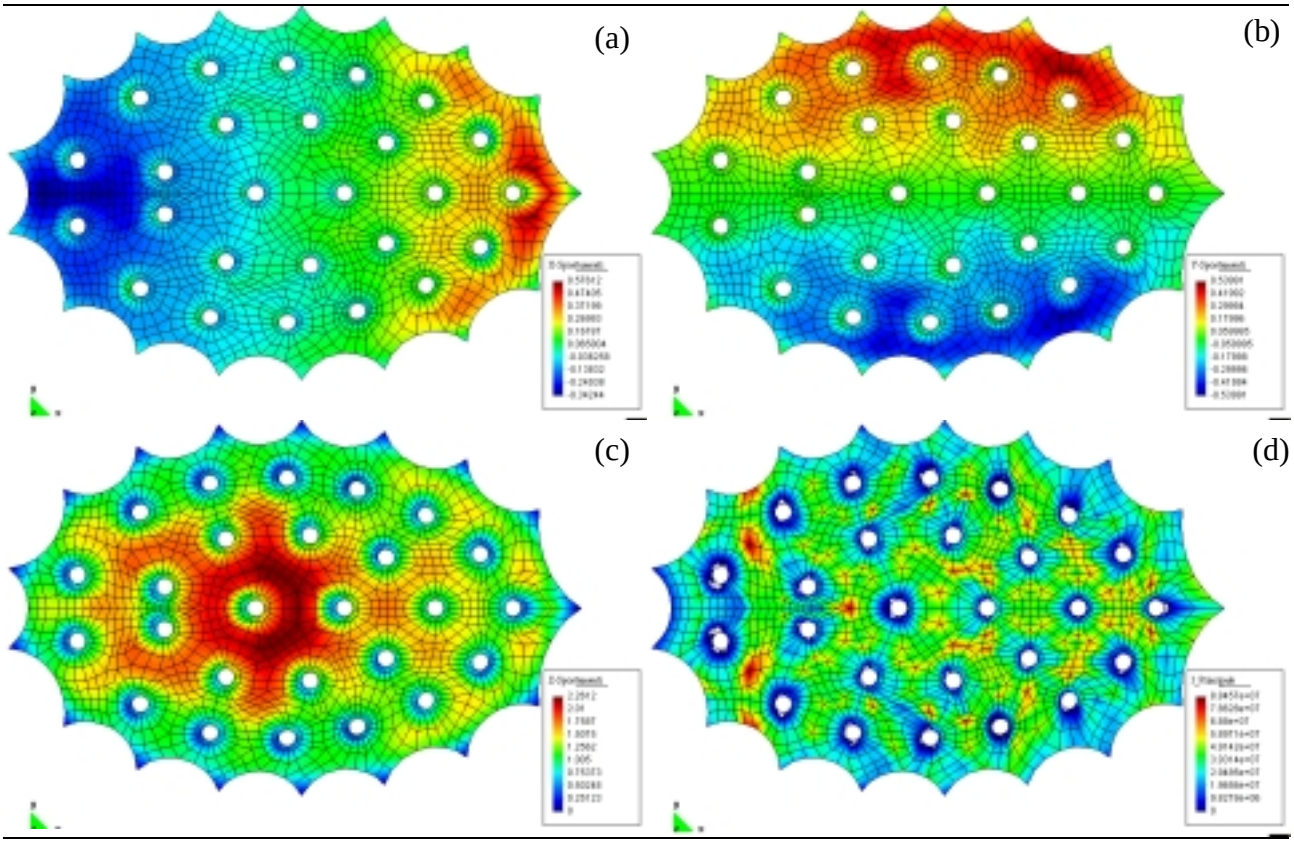

Fig. 7: wind – displacements [m] X (a), Y (b) and Z (c) and 1st principal stresses [N/mm²] (d)

The point of maximum displacement, whose deflection reaches 2.26 m, recedes from the front area observed in the case of snow towards a more central position; this is because the back no longer has the optimal behavior that it demonstrated in the case of loading due to snow.
The mapping of the displacements thus shows their tendency to increase radially from the edge towards the middle of the roof and there is no longer any onset of pocket displacements in specific areas. The 1st principal stress (Fig. 7d) reaches 140 kN/m in the internal areas coming between the cones, whereas there is generally a drop in the stress levels, that sometimes tapers down to 0, where the cones grip the membrane. There is a local "throttling" of the membrane due to the tendency of the local curvature to change sign due to the lifting: the stiffening effect attributed to the global curvature fails to contain this tendency and an inversion of the local curvature occurs. The 2nd principal stress develops in much the same way as the 1st and therefore also becomes apparent in the zeroing of the tensional state around the cones. The entity of the displacement is determined by the inadequate functioning of the principal suspension cable system in relation to decompression: their contribution to the global stiffness of the structure is soon lost as the load increases.

The markedly non-linear behavior of the membrane roofing in terms of displacement and stress is illustrated by the diagrams in Fig. 8 for loads due to snow and in Fig. 9 for the case of wind. In particular, there is clearly a drastic reduction in the 2nd principal stress in the membrane and a stiffening effect deriving from the increment in the displacements.

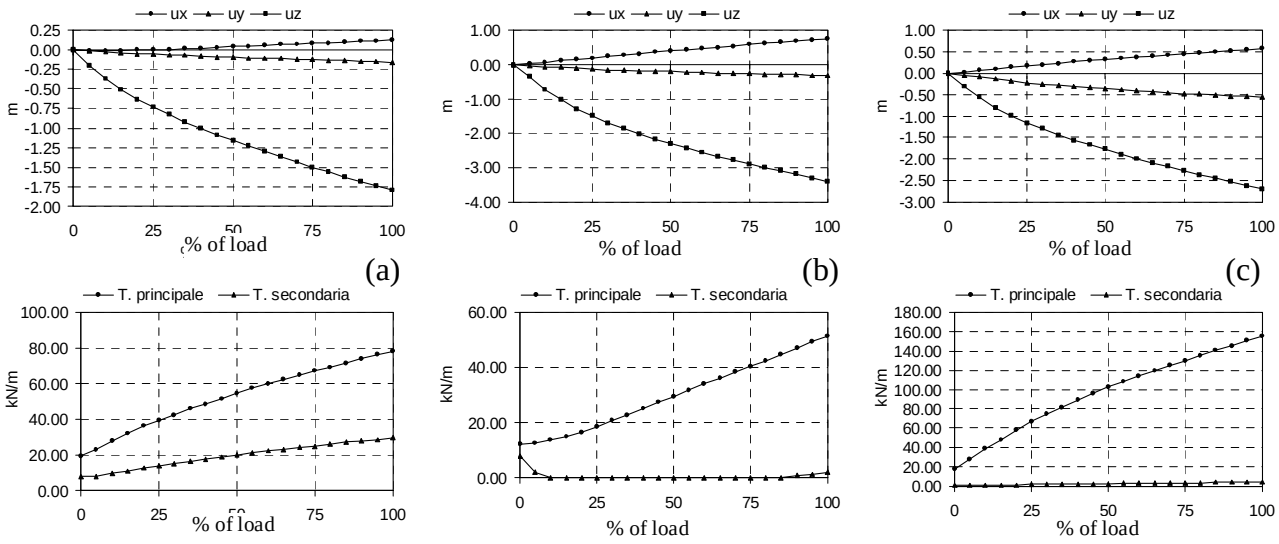

Fig. 8: Snow – membrane displacements and stresses, nodes 366 (a), 1246 (b), 1465 (c)

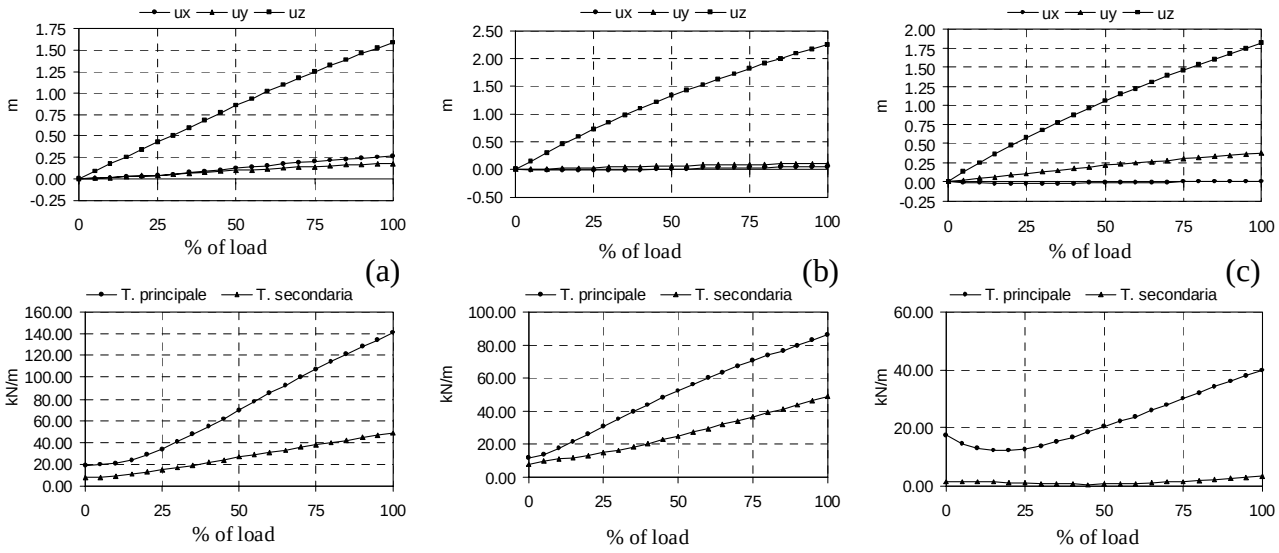

Fig. 9: Wind – membrane displacements and stresses, nodes 366 (a), 1246 (b), 1465 (c)

3.3.3 Snow: suspension and connection cables

The displacements of the principal suspension cables are due mainly to their geometrical arrangement. The cables that support the roof at the front are distinctly oblique (~ 30°-35° with respect to the horizontal) so the component normal to the cable in a vertical displacement is strong. The sub-horizontal connection cable that departs from the bottom end of the suspension cable and is connected to the perimeter ring, ensures that a normal resultant is applied to the membrane. The regimen of the major displacements that consequently dominates here becomes apparent in a non-linear displacement-load ratio that is evident in all three displacement components. Near the back of the roof, the cables become progressively more vertical and are consequently capable of responding independently and adequately to lowering forces, in addition to being better assisted in lateral movements by their respective connection cables. The displacement to load ratio is virtually linear. The midline deflection of the cables is consistently recovered (given the extension it undergoes) and the recovery mode is non-linear and asymptotic.

This aspect proved important in the interpretation of the structural response. In particular, it is evident that any vertical displacement of the head of the suspension cables at the front does not lead to an increment in the tensional state, it simply stretches the cable and reduces the deflection. The state of tension imposed by the pre-stressing is too low and the influence of the geometric response is too strong by comparison with the purely mechanical one. The resulting low tensional state combines with the poor geometrical arrangement of the principal cables with respect to the application of loads due to snow.

The diagrams of Fig. 10 show that the more slanted cables have two fundamental phases:

- the first coincides with the geometrical recovery of the deflection at the midline of the cable, characterized by a geometrically distinctly non-linear behavior;
- the second corresponds to a pseudo-linear behavior between the displacement and the entity of the load.

These two phases confirm that, in the beginning (up to about 40% of the load), the response is of a geometrically non-linear type, with the onset of major displacements, but subsequently becomes linear. The stress in the principal suspension cables increases up to values that always remain below 800 N/mm² and generally settle around 500-600 N/mm².

In the connection cables, the midline deflections tend to be recovered by the majority of the cables, except for the 5 at the tail and one cable that lies in the median part of the roofing, right on the axis of symmetry. Here again, the stress increases in almost all the cables, arriving at more than 1000 N/mm² in the first cables at the front, while the 6 previously-mentioned cables tend to be completely unloaded. The trend of the stresses remains strongly non-linear.

The perimeter cable, which works in permanent contact with the membrane, is required in this phase to perform the easiest task: it cannot have any major displacements and it reaches a maximum stress of around 500 N/mm² (and, with the exception of the front, this never exceeds 200 N/mm²).

3.3.4 Wind : suspension and connection cables

The regime of major displacements that is dominant in this case is revealed by the non-linear relationship with the load. As we move towards the back of the roof, the cables become progressively more vertical and thus, unlike the situation with the load due to snow, they are only able to respond independently and adequately to lifting up to less than 50% of the final load. Under the effect of the total load, the prestressing applied in the 0 state is almost completely lost. As the load increases, the initially-linear displacement to load ratio demonstrates a radical non-linear conversion. This behavior appears to be substantially the opposite of what happens under loads due to snow.

The deflection at the midline of the cables increases consistently, in a *quasi*-linear trend for the slanting cables Fig. 11 (a) and in a non-linear manner for the more vertical ones Fig. 11 (b)-(c).

The stress in the principal suspension cables diminishes to values of less than 100 N/mm² for the oblique cables and less than 50 N/mm² for the vertical cables, since the latter values are determined almost entirely by the self weight of the cables themselves.

The loss of tension on the suspension cables releases the membrane from the intermediate supports

and the roof, as mentioned earlier, acquires a pressostatic behavior.

In the connection cables, the midline deflections are recovered to some degree by the majority of the cables.

Similarly, the stress increases in almost all the cables, but it is only in a couple of cases that this reaches values very different from the baseline, to the point of exceeding 450 N/mm². Here again, the course of the stresses proves to be non-linear.

Another salient difference with respect to loading due to snow concerns the cable around the perimeter which continues to undergo no major displacements, but is subjected to maximum stresses in excess of 500 N/mm² along the majority of its perimeter, and not just at the front.

It is evident that in both the static load conditions studied, the roof is incapable of opposing the load with sufficient stiffness and its global structural behavior changes to acquire a function capable of withstanding the exogenous action.

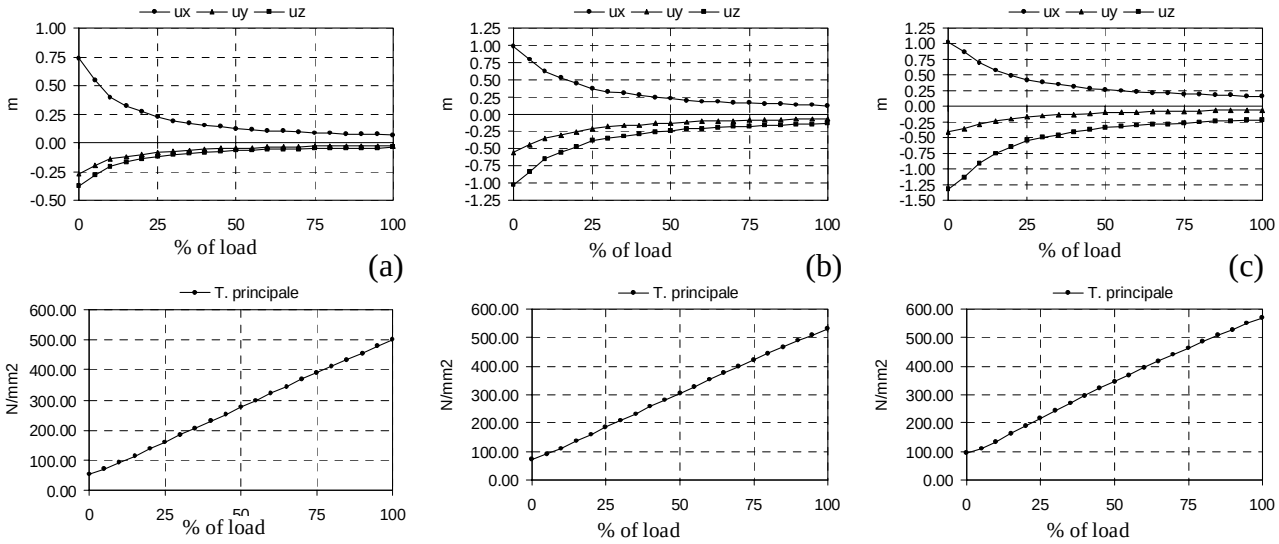

Fig. 10: Snow – suspension cables – displacements and stresses, nodes 656 (a), 1388 (b), 1738 (c)

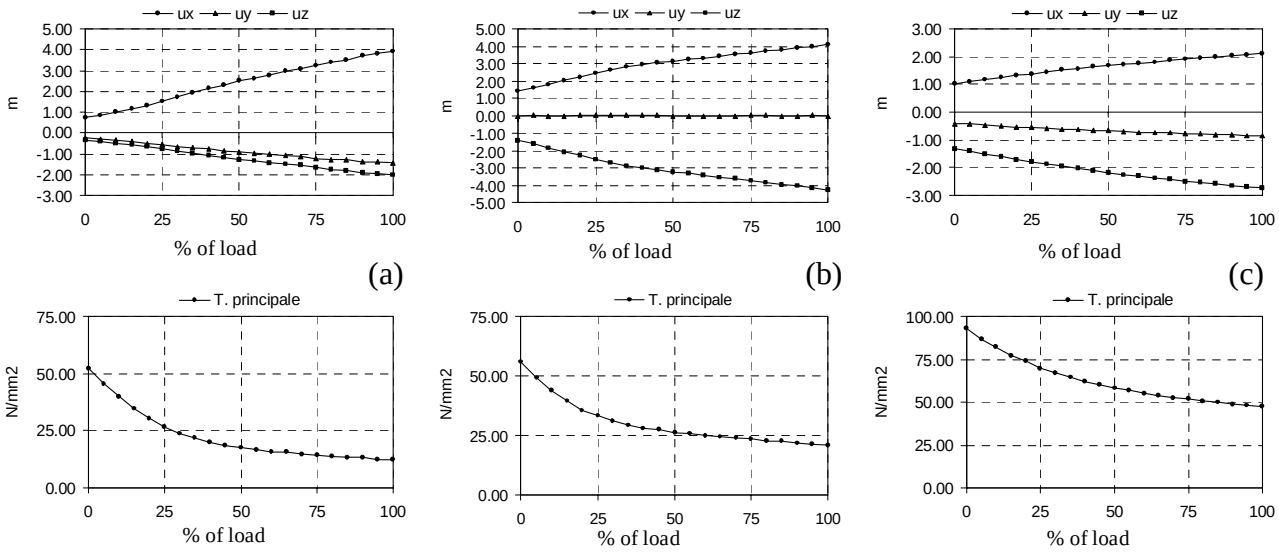

Fig. 11: Wind - suspension cables – displacements and stresses, nodes 656 (a), 1388 (b), 1738 (c)

4. Conclusions

It is particularly difficult to assess the structural response of wide-span roofing such as the structure over the Montreal Stadium. The difficulties derive essentially from the geometrically non-linear behavior typical of this type of structure and the complexity of any simulations of the loads coming to bear.

As regards the first aspect, an analysis of the stress-load and displacement-load diagrams of the roof shows that its behavior is distinctly non-linear. The major displacements that occur under the various loading conditions lead to significant variations in the roof's structural stiffness and to the zeroing of the tensional states. The linearity study is consequently not significant and has little bearing on the roof's real behavior.

The simulation of acting loads, both in the static and in the dynamic phases, calls for the use of follower forces to follow up the significant displacements.
The zeroing of the tensional states and local instability phenomena add further difficulties to the solution of the problem and make it necessary to use highly-specialized and particularly robust software. The roof reveals a low structural stiffness and a consequently excessive deformability.
The studies performed enable its structural behavior to be identified and better understood, emphasizing the problems of the two cases considered and the potential solutions to said problems.

Acknowledgements: our particular thanks go to Gustavo Bonomi for the numerical analyses performed as part of his dissertation.

5. Riferimenti Bibliografici

[1] MELCHERS R.E., "Structural reliability" Elley Horwood ltd., 1987

[2] MAJOWIECKI M., "Snow and wind experimental analysis in the design of long-span sub-horizontal structures", *Journal of Wind Engineering and Industrial Aerodynamics*, Vol. 74 - 76, 1998, 795-807.

[3] LAZZARI M., SAETTA A., VITALIANI R., "Non-linear dynamic analysis of cable-suspended structures subjected to wind actions", *Journal of Computers and Structures*, Vol. 79, N. 9, 2001, 953 - 969, March.

[4] LAZZARI M., MAJOWIECKI M., SAETTA A., VITALIANI R., "Analisi dinamica non lineare di sistemi strutturali leggeri sub - orizzontali soggetti all'azione del vento: Lo stadio di La Plata", *Proc. of the 5th National Congress of Wind Engineering*, Perugia – 13-15 September 1998.

[5] LAZZARI M., "Geometrically Non-Linear Structures Subjected To Wind Actions", Ph.D. Thesis, University of Padua, 2002

[6] KATO S., YOSHINO T., MINAMI H., "Formulation of constitutive equations for fabric membranes based on the concept of fabric lattice model", *Engineering Structures*, 21, 1999, 691 - 708.

[7] SCHWEIZERHOF K., RAMM E., "Displacement dependent pressure loads in nonlinear finite element analyses", *Computer & Structures*, Vol. 18,N. 6, 1984, 1099 – 1114.

[8] SCHWEIZERHOF K., RAMM E., "Follower force effects on stability of shells under hydrostatic loads", *J. Engng. Mech. ASCE*, Vol. 113, N. 1, 1987, 72 – 88.